Neurocomputing 311 (2018) 1–10

Contents lists available at ScienceDirect

Neurocomputing

journal homepage: www.elsevier.com/locate/neucom

Open-circuit fault diagnosis of power rectifier using sparse autoencoder based deep neural network

Lin Xu[a], Maoyong Cao[a], Baoye Song[a,*], Jiansheng Zhang[a], Yurong Liu[b], Fuad E. Alsaadi[c]

[a] College of Electrical Engineering and Automation, Shandong University of Science and Technology, Qingdao 266590, China
[b] Department of Mathematics, Yangzhou University, Yangzhou 225002, China
[c] Department of Electrical and Computer Engineering, Faculty of Engineering, King Abdulaziz University, Jeddah 21589, Saudi Arabia

ARTICLE INFO

Article history:
Received 13 February 2018
Revised 27 March 2018
Accepted 14 May 2018
Available online 19 May 2018

Communicated by Dr. Nianyin Zeng

Keywords:
Fault diagnosis
Power rectifier
Sparse autoencoder
Deep neural network
Feature extraction

ABSTRACT

This paper is concerned with the open-circuit fault diagnosis of phase-controlled three-phase full-bridge rectifier by using a sparse autoencoder-based deep neural network (SAE-based DNN). Firstly, some preliminaries on SAE-based DNN are briefly introduced to automatically learn the representative fault features from the raw fault signals. Then, a novel strategy is developed to design the structure of the SAE-based DNN, by which the depth and hidden neurons of the SAE-based DNN could be regularly determined to extract the features of input signals. Furthermore, the fault model and system framework are presented to diagnose the open-circuit fault of the three-phase full-bridge rectifier. Finally, the effectiveness of the developed novel strategy is verified by the results of simulation experiments, and the superiority of the novel SAE-based DNN is evaluated by comparing with other frequently used approaches.

1. Introduction

With the rapid development of power electronics in recent decades, power electronic converters have been widely used in various engineering fields, e.g. high-voltage DC transmission, renewable energy, suppression of power harmonics, high power electrolysis, driving system of inverter-fed motor, electric vehicle and industrial robotics [41], etc. Power rectifier is one of the most important power electronic converters, which is not only used directly for AC to DC conversion, but also acts as the front half of the rectifying and inverting systems. The normal operation of power electronic switches is one of the most important factors related to the reliability and efficiency of the power electronic system. However, because of the exposure to poor working environments, the rectifier is prone to suffer critical failures because of device aging, overloading and unexpected operating conditions, etc. It has been reported that about 38% of the faults of power electronic system are due to failures of power electronic switches [39]. Therefore, the fault diagnosis of rectifier, which is extremely necessary to shorten the system downtime and enhance the system reliability, has become a hot topic during the last decades [16,24,40].

Most of the rectifier faults would occur on the power electronic switches, mainly in the form of short circuit (SC) and open circuit (OC) [23,26]. The SC fault, which is usually caused by several abnormal operating conditions (e.g. overvoltage and insulation damage), would lead to extreme high current in the power system. Then, the overcurrent would trigger the action of protection system (e.g. the fuse of circuit) and result in the OC fault in the end. While, the OC fault usually would not make the system shut down immediately,touch the alarm of the protection system, but it would gradually degrade the performance of the rectifier, and finally lead to faults of other components and even further worse failures if no fault diagnosis system is available [2]. Therefore, the diagnosis of open-circuit fault is a critical issue for reliable operation of the power electronic rectifier.

To deal with the problem of open-circuit fault diagnosis, several approaches have been proposed in recent years. There are mainly three methods used for fault diagnosis of power rectifier, i.e. model-based methods, data-based methods, and artificial intelligent methods. Generally, model-based methods have been widely used in fault detection and isolation of industrial systems, but these methods are poor in robustness and sensitive to parameters. So that, data-based methods and artificial intelligent methods are becoming more and more popular in the fault diagnosis of power rectifier in recent years [7,8]. For example, a data-driven-based approach has been presented in [2], where the line-to-line voltages are measured as input signals, and the feature extraction

* Corresponding author.
E-mail addresses: my-cao@263.net (M. Cao), songbaoye@gmail.com (B. Song).

https://doi.org/10.1016/j.neucom.2018.05.040
0925-2312/

is conducted by fast Fourier transform (FFT). Then, the principal component analysis (PCA) is used to reduce the dimensions of the feature samples, and finally a Bayesian network (BN) is employed to diagnose the different fault modes of the system. A new algorithm has been proposed in [4], where a fault space is defined based on the extracted fault features, and the experimental results show that the new algorithm is superior to several traditional approaches, such as expert system and fuzzy logic. In [9], a hybrid technique has been developed for the diagnosis and classification of open-circuit faults, whose features are extracted by using the integrated discrete wavelet transform (DWT) and PCA. Afterwards, the fault classification is implemented with a fuzzy logic system and relevance vector machine (RVM), where several intelligent optimization algorithms, e.g. evolutionary particle swarm optimization (EPSO) and cuckoo search optimization (CSO), are incorporated to enhance the fault diagnosis system. To overcome the limitations of traditional neural network (NN), a novel neural network group approach has been proposed to diagnose the open-circuit faults of the electronic power switches [22]. In the proposed approach, the fault samples are divided into different grades according to the occurring frequencies of the faults, and then the samples corresponding to more frequently occurring faults would be learnt by more sub neural networks. In [36], an integrated method combining PCA and support vector machine (SVM) has been put forward for the open-circuit fault diagnosis of three-phase full-bridge rectifier, where the fault features are extracted by PCA from raw voltage data and the SVM classifier is applied to identify the fault types.

It should be noted that the open-circuit fault diagnosis of power electronic rectifier is a typical classification problem, and the methodologies mentioned above usually involve two steps to diagnose the faults [33]. Firstly, the fault features are extracted from the raw voltage/current data via time- or frequency-domain approaches, e.g. PCA, FFT and DWT, etc. Then, the diverse fault modes are identified through classifying the extracted features by using a sort of classification algorithm, e.g. NN, SVM and BN, etc. Nevertheless, these methods have not been widely used in practice, because it is hard to achieve satisfying diagnosis accuracy [37].

As is well known, feature representation is the key to the classification problem [3,13]. In conventional fault diagnosis methods, the diagnostic performance heavily depends on the manually designed feature extraction algorithms, i.e. the representative features could not be extracted from the raw signals automatically [14,27]. So that the quality of the extracted features is largely related to the professional expertise of the specific diagnostic issues, and it is really a costly and laborious work to select the most suitable features to diagnose the faults. To handle above mentioned weaknesses of traditional methods, many researchers have been stirred to explore new approaches to acquire the representative features automatically, and hence improve the performance of fault diagnosis. Deep neural network (DNN) is one of the most popular machine learning algorithms in nowadays, and has been extensively utilized to various fields, including fault diagnosis [12,15,20,42]. For example, a sparse autoencoder (SAE) based DNN approach has been presented to diagnose induction motor fault, where the strategies of denoising coding, partial corruption and dropout are involved to strengthen the robustness of feature representation and prevent the overfitting of neural network [32]. In [17], a multimodal deep support vector classification (MDSVC) method has been proposed for gearbox fault diagnosis. The vibration signals of gearbox are firstly divided into multi modalities, then a Gaussian–Bernoulli deep Boltzmann machine (GDBM) is applied to learn the feature representations of each modalities, and finally a support vector classifier is adopted to carry out the fault pattern recognition. In [38], deep learning neural network has been used for the fault diagnosis of power system, in which the SAE is trained to extract the hidden features in different dimensions.

To our knowledge, the sparse autoencoder based deep neural network (SAE-based DNN) has not been widely used in the fault diagnosis of power electronic circuits except for few scattered results [5,6]. In this paper, the open-circuit fault diagnosis of phase-controlled three-phase full-bridge rectifier is investigated by using the SAE-based DNN. The output voltage of the rectifier is measured and fed into the deep sparse autoencoder, then the fault features are automatically extracted and stored in the hidden neurons. To select the depth and hidden neurons of the deep sparse autoencoder, a novel strategy is proposed to design the structure of the SAE-based DNN. Finally, the distinct faults are identified by using softmax regression of the deep neural network, and the superior diagnosis accuracy and other benefits of the fault diagnosis system have been verified by simulation results. The main contributions of this paper could be summarized as follows. *(1) A sparse autoencoder based deep neural network is firstly used for the open-circuit fault diagnosis of phase-controlled three-phase full-bridge rectifier, whose fault features could be automatically learnt from the raw voltage signals by using the deep sparse autoencoder. (2) A novel strategy is proposed to design the structure of the sparse autoencoder based deep neural network, by which the depth and hidden neurons of the deep sparse autoencoder could be regularly selected by using an uncomplicated optimization algorithm; (3) The simulation model of fault diagnosis system is established and exhibits a superior performance than the frequently used approaches according to comprehensive simulation experiments.*

The rest of this paper is organized as follows. In Section 2, the sparse autoencoder based deep neural network is briefly introduced, and then a novel strategy is presented to design the structure of the SAE-based DNN. Section 3 details the fault model and system framework for fault diagnosis of three-phase full-bridge rectifier. In Section 4, the simulation results are discussed and evaluated by comparing with two of the frequently used approaches. Finally, conclusions are summarized and future works are drawn in Section 5.

2. Sparse autoencoder based deep neural network

2.1. Sparse autoencoder

An autoencoder (AE) is a symmetrical three-layer neural network, which has been frequently used for the unsupervised feature learning of original data [20,42]. By minimizing the errors between the input data and its reconstructions, the output of the hidden layer could be taken as a meaningful feature representation of the unlabeled data. As shown in Fig. 1, an autoencoder is implemented in two steps, i.e. encoding and decoding.

In the step of encoding, the unlabeled data vector $\{\mathbf{x}_i\}_{i=1}^{M}$, where $\mathbf{x}_i \in \Re^{N\times 1}$, is put into the input layer of the neural network, and then the output vector of the hidden layer $\mathbf{h}_i$ is calculated by the following nonlinear activation function:

$$\mathbf{h}_i = f(\mathbf{x}_i) = sigmoid(\mathbf{W}_1\mathbf{x}_i + \mathbf{b}_1), \tag{1}$$

where $\mathbf{W}_1$ and $\mathbf{b}_1$ indicate respectively the weight matrix and bias vector of the encoder; $sigmoid(\cdot)$ represents the sigmoid function, which is calculated as follows:

$$sigmoid(x) = \frac{1}{1+e^{-x}}. \tag{2}$$

In the step of decoding, the hidden vector $\mathbf{h}_i$ is converted back to reconstruct the input vector (denoted as $\hat{\mathbf{x}}_i$) by the similar nonlinear activation function:

$$\hat{\mathbf{x}}_i = g(\mathbf{h}_i) = sigmoid(\mathbf{W}_2\mathbf{h}_i + \mathbf{b}_2), \tag{3}$$

where $\mathbf{W}_2$ and $\mathbf{b}_2$ indicate respectively the weight matrix and bias vector of the decoder. The reconstruction error, which is also taken

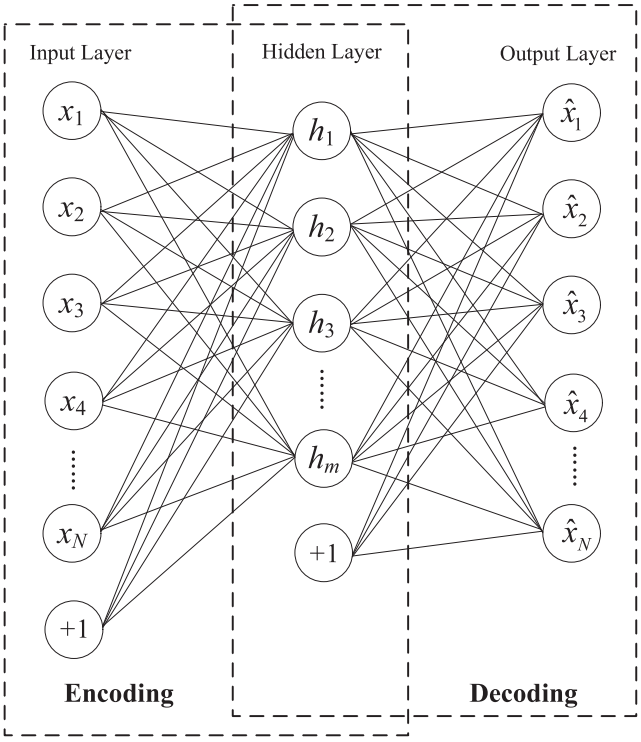

Fig. 1. Structure of an autoencoder.

as the cost function to be minimized, could be defined as follows:

$$J_{\mathrm{AE}} = \frac{1}{2M}\sum_{i=1}^{M}\|\mathbf{x}_i - \hat{\mathbf{x}}_i\|_2^2 + \frac{\lambda}{2}\sum_{l=1}^{n_l-1}\sum_{j=1}^{s_l}\sum_{i=1}^{s_{l-1}}(W_{ij}^l)^2, \tag{4}$$

where M denotes the sample size of the training set; λ denotes the regularization parameter that regulates the weight of the two terms of Eq. (4) and helps to prevent the phenomenon of overfitting; n_l denotes the layers of the network, and s_l denotes the neurons of layer l.

To achieve better performance of AE, a sparsity constraint is imposed on the cost function to realize the sparse representation of features. So that, the reconstruction error of the sparse autoencoder (SAE) with sparsity penalty term is redefined as follows:

$$J_{\mathrm{SAE}} = J_{\mathrm{AE}} + \beta\sum_{j=1}^{K}\mathrm{KL}(\rho\|\hat{\rho}_j), \tag{5}$$

where β is a coefficient to control the weight of the sparsity penalty term; K denotes the size of the neurons in the hidden layer; $\mathrm{KL}(\cdot)$ stands for the Kullback-Leibler divergence [34], which is employed to promote the sparsity of the hidden feature $\mathbf{h}_i$ and can be defined as follows:

$$\mathrm{KL}(\rho\|\hat{\rho}_j) = \rho\log\frac{\rho}{\hat{\rho}_j} + (1-\rho)\log\frac{1-\rho}{1-\hat{\rho}_j} \tag{6}$$

where $\hat{\rho}_j = \frac{1}{M}\sum_{i=1}^{M} h_j^i$ denotes the average activation of the jth hidden neuron of the neural network with input vector $\mathbf{x}_i$; and ρ denotes the predefined sparsity parameter, i.e. the expected average activation of hidden neurons, which acts as a sparsity constraint. It is clearly that the penalty function $\mathrm{KL}(\rho\|\hat{\rho}_j) = 0$ if $\hat{\rho}_j = \rho$, otherwise, $\mathrm{KL}(\rho\|\hat{\rho}_j)$ will increase rapidly with the growing divergence between $\hat{\rho}_j$ and ρ.

In the training of SAE, the backpropagation (BP) algorithm is usually exploited to optimize the parameters of the neural network by minimizing the cost function of Eq. (5), where the weight and bias are updated iteratively as follows:

$$W_{ij}^l = W_{ij}^l - \alpha\frac{\partial}{\partial W_{ij}^l}J_{\mathrm{SAE}}, \tag{7}$$

$$b_i^l = b_i^l - \alpha\frac{\partial}{\partial b_i^l}J_{\mathrm{SAE}}, \tag{8}$$

where α denotes the learning rate; l denotes the lth layer of the network; i and j indicate respectively the ith and jth neurons of two adjacent layers.

2.2. Deep sparse autoencoder

Deep sparse autoencoder (DSAE) is a deep neural network constructed by stacked sparse autoencoders, and several classifiers (e.g. Softmax and SVM) could be employed to tackle with the issues of pattern classification. As shown in Fig. 2, the output features of the hidden layer could be accepted as the input of the next layer after the pre-training of each autoencoder using the approach explained above. Then, given the expected labels, the parameters of the whole deep neural network could be fine-tuned by using the BP algorithm again, where the cost function could be expressed as follows:

$$J_{\mathrm{DSAE}}(\mathbf{W}_L, \mathbf{W}_{1,k}|_{k=1}^{L-1}, \mathbf{b}_{1,k}|_{k=1}^{L-1}) = \arg\min_{\mathbf{W}_L,\mathbf{W}_{1,k},\mathbf{b}_{1,k}} \frac{1}{2M}\sum_{i=1}^{M}\|\,\mathbf{y}_i - g_L(f_L(\mathbf{h}_i^{L-1}))\,\|_2^2 \tag{9}$$

where L denotes the total number of layers; $\mathbf{h}_i^{L-1} = f_{L-1}(f_{L-2}(\cdots f_1(\mathbf{x}_i)))$ stands for the output feature vector of the (L−1)th hidden layer; $\mathbf{y}_i$ indicates the label vector of $\mathbf{x}_i$; $\mathbf{W}_L$ represents the weight matrix of the last layer, $\mathbf{W}_{1,k}$ and $\mathbf{b}_{1,k}$ represent respectively the weight matrix and bias vector of the kth layer of the deep neural network.

Remark 1. Nowadays, various classification algorithms could be utilized to classify the feature patterns extracted from the hidden layers of DSAE. Besides, several optimization algorithms could be exploited for the pre-training of each autoencoder and fine-tuning of the deep neural network, e.g. gradient descent based BP algorithm [25], intelligent optimization algorithms such as artificial bee colony [1] and particle swarm optimization [11], etc. *However, two significant problems of the deep neural network, i.e. how to select the suitable number of featured neurons of each autoencoder and how to identify the proper depth of the deep neural network, are still techniques of expertise and need to be explored further. So that, a novel strategy has been developed in the following section to design the structure of the SAE-based DNN.*

2.3. A novel strategy to design the structure of SAE-based DNN

It is well known that the SAE-based DNN is actually a neural network with several layers. However, the strategy to design the structure of the deep neural network is still an open problem being explored. Usually, the hidden neurons of an autoencoder are less than the ones of input layer, which means that the compressed features of input signals could be expressed by the outputs of hidden neurons.

In this section, a novel strategy has been proposed to design the neuron number of the hidden layers, and then the layer number of the neural network could also be determined. Suppose there are N neurons in the input layer as shown in Fig. 3, then the neuron number of the first hidden layer is taken as 2^n, where n is selected as the maximum integer subjecting to $2^n \le N$ (e.g., n equals 6 for N=100). In the second hidden layer, the neuron number is taken as 2^{n-1}, then 2^{n-2} hidden neurons are remained in the third hidden

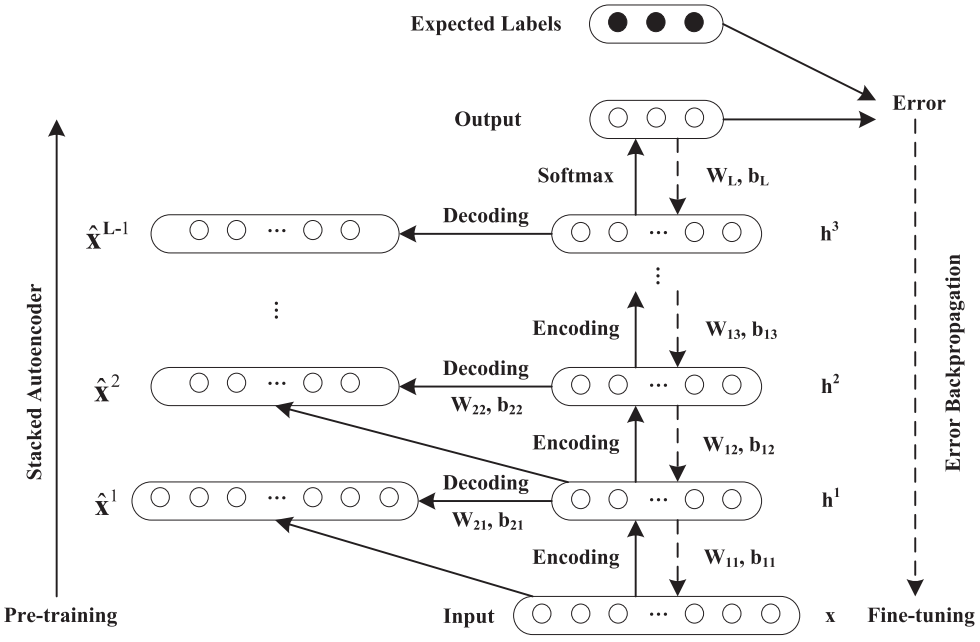

Fig. 2. Structure of deep sparse autoencoder.

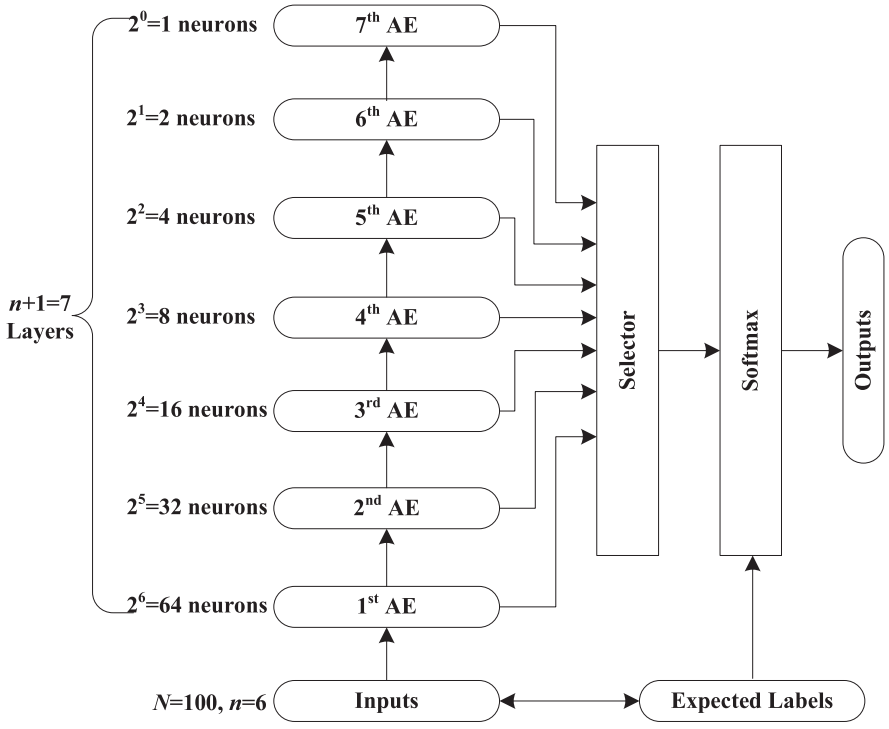

Fig. 3. Novel structure of SAE-based DNN in case of N=100.

layer, and the neuron number could be selected with this rule in the next hidden layers iteratively. Finally, the compressed features of certain hidden layer could be selected to feed into a Softmax classifier of the deep neural network. In Fig. 3, a selector is employed to choose the hidden layer, from which the hidden features are extracted for the final feature classification. Usually, this is not a complicated optimization problem under the index of classification accuracy.

Remark 2. In the proposed strategy, the neuron number of the first hidden layer is chosen as n power of 2 where n is the maximum integer subjecting to $2^n \leq N$, and half of the hidden neurons would be remained in the next hidden layer. With the descending of neurons in the hidden layers iteratively, there will be only one neuron ($2^0 = 1$) in the last hidden layer of the deep sparse autoencoder, so the maximum depth of the deep sparse autoencoder is limited to $n + 1$. Generally, the number of neurons fed into the Softmax should be greater than the output classifications of the classifier. Therefore, by selecting an appropriate hidden layer to extract the features of input signals, the structure of the deep neural network could be determined by using this novel strategy.

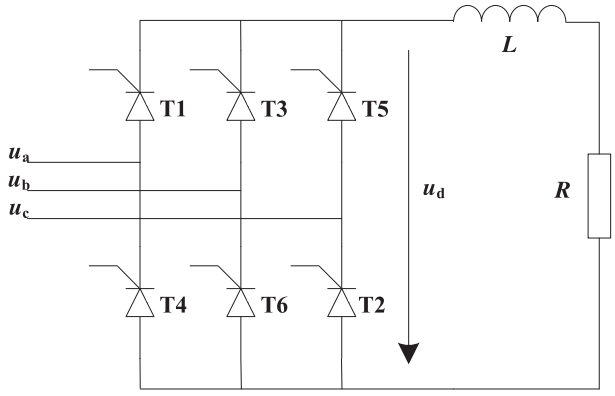

Fig. 4. System model for fault diagnosis of three-phase full-bridge rectifier.

3. Open-circuit fault diagnosis of three-phase full-bridge rectifier

3.1. Fault model of three-phase full-bridge rectifier

In this paper, the open-circuit fault diagnosis of phase-controlled three-phase full-bridge rectifier is concerned by using the SAE-based DNN. The system model for fault diagnosis is shown as Fig. 4. Because of the extensive applications of thyristors in high-voltage and high-power converter fields, the destroyed thyristors are taken as examples to simulate the open-circuit faults of power switches in the three-phase full-bridge rectifier. Considering the practical fault conditions and the complexity of the system, the rectifier is assumed to be operated in phase controlled mode and no more than two switches (i.e. thyristors) are broken at the same time. Therefore, the switch faults could be divided as the following four types:

Fault type I: One of the switches is broken, which includes the following fault cases, i.e. T1 broken, T2 broken, T3 broken, T4 broken, T5 broken and T6 broken.

Fault type II: Two switches of the same bridge get broken, which includes the fault cases of T1 and T4 broken, T3 and T6 broken, T5 and T2 broken.

Fault type III: Two switches of different bridges from same sides are broken, which also includes six fault cases, e.g. T1 and T3 broken, T3 and T5 broken, T4 and T2 broken, etc.

Fault type IV: Two switches of different bridges from different sides are broken, which includes six fault cases, e.g. T1 and T6 broken, T3 and T2 broken, T4 and T5 broken, etc.

The fault codes of all fault cases are listed in Table 1, where each fault is encoded into a 6-bit binary number. The codes of faults would be utilized as the output labels of the deep neural network, so the faults could be identified by using a classifier with six output neurons.

3.2. System framework for fault diagnosis

In this paper, the fault features of three-phase full-bridge rectifier are learnt from the unlabeled data by using an unsupervised learning approach. The training data are normalized firstly and then used to train the DSAE in the following steps:

1) Construct the deep sparse autoencoder according to the proposed approach explained above.
2) Initialize the weights and biases of each autoencoder and set the parameters such as learning rate, sparse rate and denoising rate, etc.
3) Compute the cost function of each autoencoder according to Eqs. (4)–(6).

Table 1
Fault encoding of three-phase full-bridge rectifier.

Fault Class	Fault	Fault code
Normal	No	001001
Fault type I	T1	010001
	T2	010010
	T3	010011
	T4	010100
	T5	010101
	T6	010110
Fault type II	T1, T4	011001
	T3, T6	011010
	T5, T2	011011
Fault type III	T1, T3	100001
	T1, T5	100010
	T3, T5	100011
	T4, T6	100100
	T2, T4	100101
	T2, T6	100110
Fault type IV	T1, T6	101001
	T1, T2	101010
	T3, T4	101011
	T3, T2	101100
	T5, T4	101101
	T5, T6	101110

4) Update the weights and biases of each autoencoder according to Eqs. (7) and (8).

After the training of each sparse autoencoder, the labeled fault voltage data are used to train the SAE-based DNN in the following steps:

1) Initialize the SAE-based DNN with the parameters acquired from the training of DSAE.
2) Extract the fault features from one of the hidden layers and put them into a Softmax classifier.
3) Compute the cost function of the deep neural network according to Eq. (9) and the output labels listed in Table 1.
4) Update and fine-tune the SAE-based DNN based on the BP algorithm expressed by Eqs. (7) and (8).

Finally, the selector in Fig. 3 is employed to choose the most appropriate hidden layer according to the average classification accuracy, and the output features of the selected hidden layer are fed into the Softmax classifier. Then, the fault test data could be used to check the effectiveness of the diagnostic system for the fault diagnosis of three-phase full-bridge rectifier. The framework of the diagnostic system could be shown as Fig. 5.

4. Simulation results and discussions

4.1. Simulation model and setup

To verify the effectiveness of the SAE-based DNN for fault diagnosis of three-phase full-bridge rectifier, an simulation model is constructed in MATLAB/Simulink as illustrated in Fig. 6. The output voltage signals in fault conditions can be measured by the `Voltage Measurement` module under different fault conditions set by modules of `Fault Type` and `Fault Num`. The output voltage signals of the simulation model are collected with the sampling frequency of 5 kHz under a supply frequency of 50 Hz, and the voltage data of steady state are memorized in the 500 dimensional data vectors for further fault feature learning and fault classifying. To simulate the actual operating conditions of power supply, random noises are added into the sampled data vectors and 100 data vectors are remained for each fault mode. These data are randomly selected for training and testing of the SAE-based DNN,

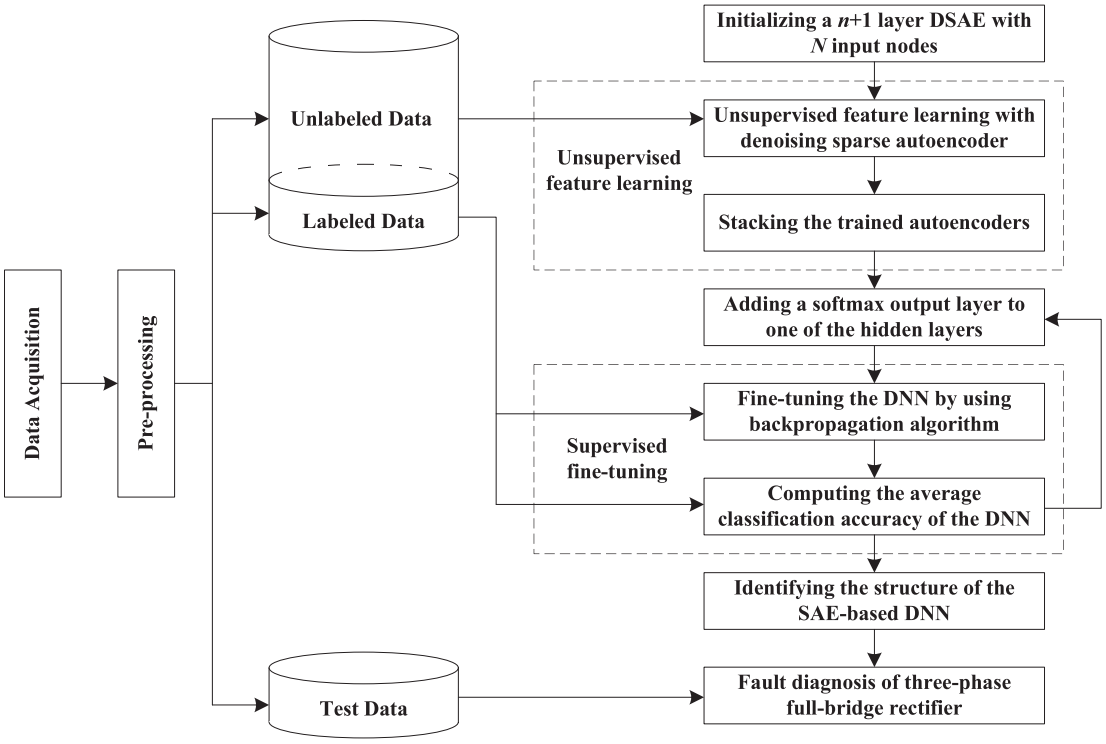

Fig. 5. Framework of the fault diagnostic system.

Table 2
Confusion matrix of SAE-based DNN (%).

	001001	010001	010010	011001	011010	100001	100010	101001	101010
001001	100	0	0	0	0	0	0	0	0
010001	0	100	0	0	0	0	0	0	0
010010	0	0	100	0	0	0	0	0	0
011001	0	0	0	100	0	0	0	0	0
011010	0	0	0	0	100	0	0	0	0
100001	0	0	0	0	0	100	0	0	0
100010	0	0	0	0	0	0	100	0	0
101001	0	0	0	0	0	0	0	100	0
101010	0	0	0	0	0	0	0	0	100

Table 3
Confusion matrix of PCA-BPNN (%).

	001001	010001	010010	011001	011010	100001	100010	101001	101010
001001	100	0	0	0	0	0	0	0	0
010001	0	0	0	0	0	0	0	100	0
010010	0	0	100	0	0	0	0	0	0
011001	0	0	0	100	0	0	0	0	0
011010	0	0	0	0	100	0	0	0	0
100001	0	0	0	0	0	100	0	0	0
100010	0	0	0	0	0	0	100	0	0
101001	0	100	0	0	0	0	0	0	2
101010	0	0	0	0	0	0	0	0	98

and the main parameters are set as follows: input neurons of the DSAE is set as 500; output neurons of the SAE-based DNN is set as 6; weight regularization λ is set as 0.001; sparsity proportion ρ is set as 0.05 and sparsity weight β is set as 4.

To compare with the SAE-based DNN, the simulation experiments based on PCA-BPNN and FFT-BPNN approaches are implemented to evaluate the performances of the proposed approach. In PCA-BPNN, the principal components of fault voltage signals are extracted by using PCA at first, and then the labeled data are fed into BP neural network (BPNN) for fault classification. In FFT-BPNN, an FFT preprocessing of fault voltage data is firstly conducted, and then the features of harmonic components are used for the fault diagnosis based on BPNN. The results of simulation experiments are detailedly presented and discussed in the following section.

4.2. Results and discussions

It should be noted that there are 22 fault types (including the normal type) in the diagnostic system and the triggering angles of the rectifier can be regulated according to the control signals of the system. Without loss of generality, two cases of each fault type with triggering angle of 30° are concerned in the following results and discussions. The normalized typical voltage signals of these fault cases without noises are shown in Fig. 7, where there

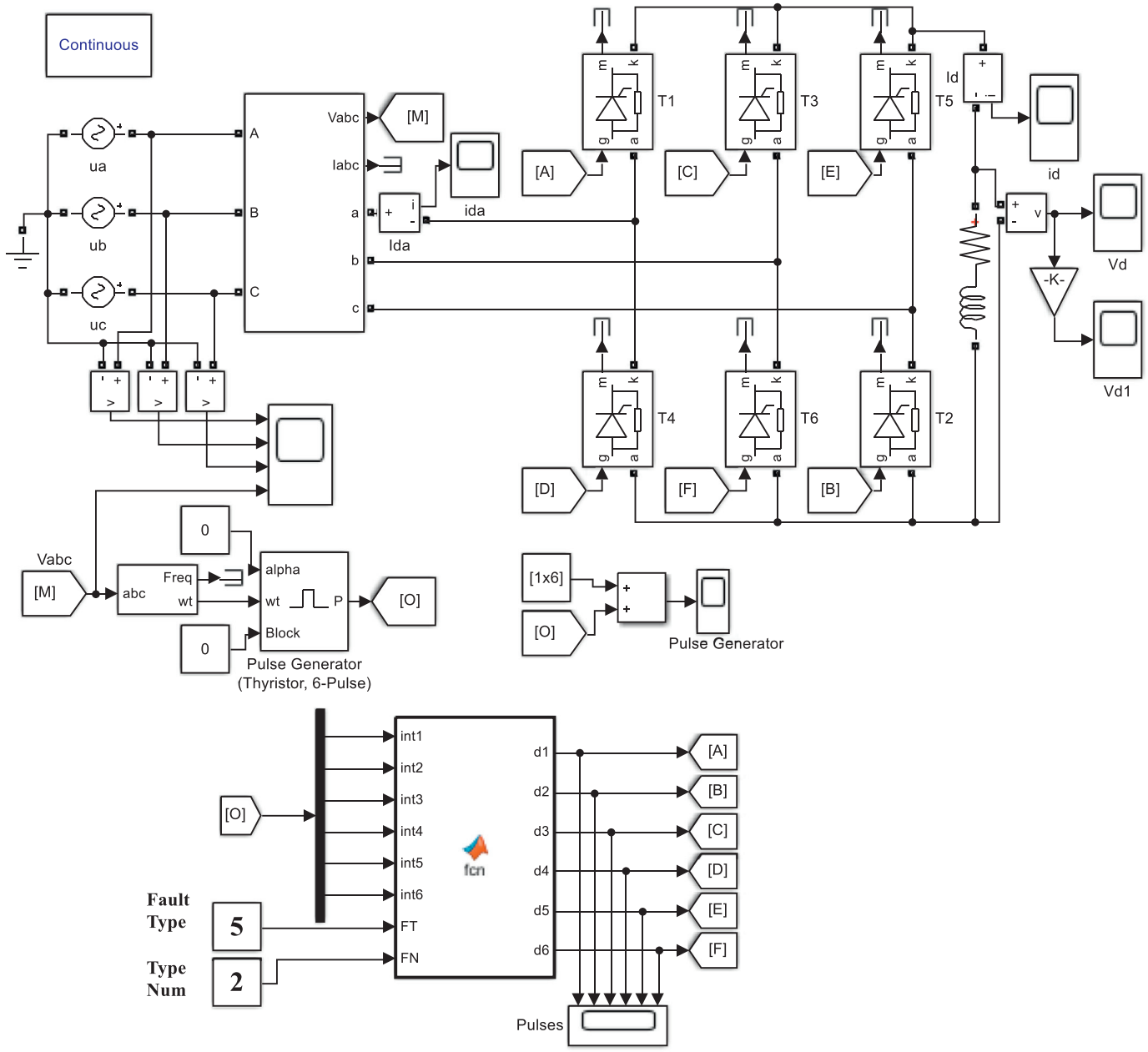

Fig. 6. Simulation model for fault diagnosis of three-phase full-bridge rectifier.

Table 4
Confusion matrix of FFT-BPNN (%).

	001001	010001	010010	011001	011010	100001	100010	101001	101010
001001	100	0	0	21	0	0	0	0	0
010001	0	100	0	44	0	0	0	0	0
010010	0	0	100	1	0	0	34	0	1
011001	0	0	0	12	1	10	0	0	0
011010	0	0	0	11	76	0	0	43	0
100001	0	0	0	11	23	89	0	0	0
100010	0	0	0	0	0	0	66	0	0
101001	0	0	0	0	0	0	0	57	22
101010	0	0	0	0	0	1	0	0	77

are 500 sampling points for each fault case and the fault cases are indicated by using the fault codes of Table 1.

For the fault diagnostic problem of this paper, the input fault voltage signals are 500 dimensional data vectors, so that there are 256 (2^8) neurons in the first hidden layer of the SAE-based DNN, and the maximum hidden layers of the DSAE would be 9 ($8+1$) according to the strategy proposed in Section 2.3. To determine the structure of the SAE-based DNN, the fault features of the input signals are extracted from different hidden layers respectively and then put into the Softmax classifier to acquire the accuracies of the

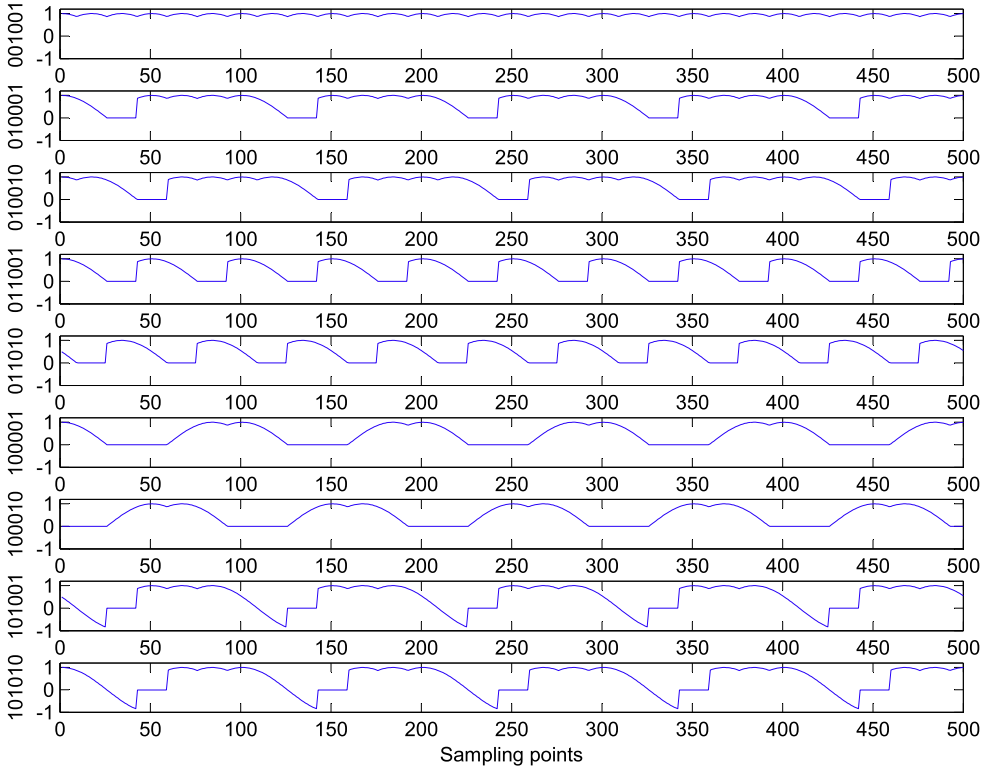

Fig. 7. Normalized typical voltage signals of fault cases without noises.

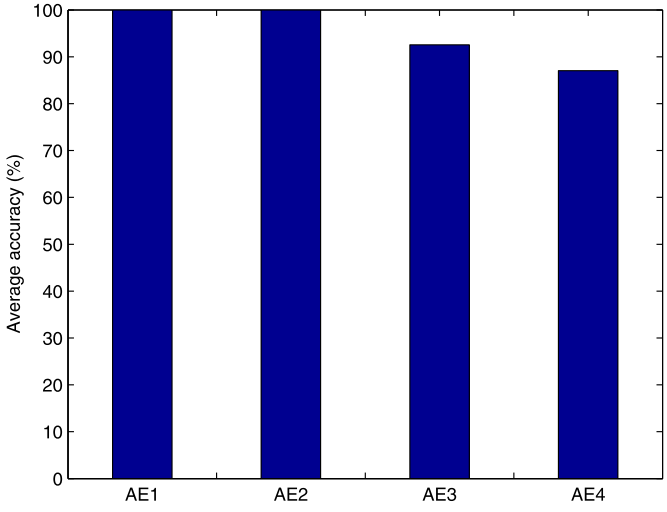

Fig. 8. Average accuracies with fault features extracted from different hidden layers.

fault diagnosis. Fig. 8 illustrates the average accuracies of the fault diagnostic system (i.e. 100%, 100%, 92.55% and 87.05%) after several simulation experiments, where AE1 to AE4 indicate respectively 1st to 4th hidden layers of the DSAE from which the features are extracted, and the cases of more than 4 hidden layers have been disregarded because of their poor average accuracies. This can be explained by the fact that there should be at most 4 hidden layers of the DSAE for the discussed diagnostic problem, because the number of neurons fed into the Softmax classifier should be greater than the number of output classification, i.e. $2^{8-3} > 22$. In addition, as observed in Fig. 8, the average accuracies start to descend from 100% when the fault features are extracted from 3rd hidden layer. This could be explained that the dimension of the features to fully discriminate the fault modes should be greater than 2^{8-2}, so we use the fault features extracted from 2nd hidden layer in the following discussions.

Furthermore, to compare the performance of SAE-based DNN with frequently used PCA-BPNN and FFT-BPNN approaches (see e.g. [2] and [22] for more details), the confusion matrices of them are listed in Tables 2–4, respectively. It can be observed that the SAE-based DNN could achieve excellent performance with the accuracy of 100% for each fault mode, owing to the powerful feature learning and expressing ability of SAE-based DNN. Comparatively, the PCA-BPNN, which could also extract signal features automatically, achieves a discouraging accuracy of 77.6% because of a few serious confusions, e.g. the fault mode of 010001 is completely misclassified as the fault mode of 101001 and vice versa. While, FFT-BPNN, which is a manual feature extraction approach, would unsurprisingly achieve low accuracy of 75.2% because of a lot of confusions of the fault modes shown in the table. Based on the above discussions, it can be concluded that the SAE-based DNN could outperform the approach of PCA-BPNN and FFT-BPNN due to its robust feature learning ability. Besides, it is worthy mentioning that the similar conclusions would be achieved when other fault cases and variable triggering angles are used for the simulation experiments of fault diagnosis.

5. Conclusions

In this paper, the open-circuit fault diagnosis of phase-controlled three-phase full-bridge rectifier is investigated by using an SAE-based DNN, which could automatically learn the representative fault features from the raw signals and achieve excellent accuracy of classification. Particularly, a novel strategy has been proposed to design the structure of the SAE-based DNN, by which the depth and hidden neurons of the DSAE could be regularly selected to extract the features of input signals. The effectiveness of the proposed strategy could be verified by the results of several sim-

ulation experiments, and the superiority of the proposed approach is evaluated by comparing with other frequently used approaches.

The parameters and structure of the SAE-based DNN are manually determined in this paper. In future works, we will use the intelligent optimization algorithms (e.g. [29–31]) to automatically choose the optimized parameters and extend the application of the proposed SAE-based DNN to more complicated systems, , such as fault detection and isolation of mobile robot, unmanned aerial vehicle, and autonomous underwater vehicle, etc [10,18,19,21,28,35,43–46].

Acknowledgments

This work was supported in part by the National Natural Science Foundation of China under Grant 61703242 and 61603221, the Higher Educational Science and Technology Program of Shandong Province of China under Grant J14LN34, and the National Natural Science Foundation of Shandong Province under Grant ZR2016FB11.

References

[1] H. Badem, A. Basturk, A. Caliskan, M.E. Yuksel, A new efficient training strategy for deep neural networks by hybridization of artificial bee colony and limited-memory BFGS optimization algorithms, Neurocomputing 266 (2017) 506–526.
[2] B. Cai, Y. Zhao, H. Liu, M. Xie, A data-driven fault diagnosis methodology in three-phase inverters for PMSM drive systems, IEEE Trans. Power Electron. 32 (7) (2017) 5590–5600.
[3] Y. Bengio, A. Courville, P. Vincent, Representation learning: a review and new perspectives, IEEE Trans. Pattern Anal. Mach. Intell. 35 (8) (2013) 1798–1828.
[4] C. Cai, J. Du, R. Gao, W. Liu, A fault diagnosis method used for the three--phase full-bridge rectifier circuit, in: Proceedings of International Symposium on Computer, Consumer and Control, 2016, pp. 1101–1105.
[5] J. Cui, J. Tang, G. Shi, Z. Zhang, Generator rotating rectifier fault detection method based on stacked auto-encoder, in: Proceedings of IEEE Workshop on Electrical Machines Design, Control and Diagnosis, 2017, pp. 256–261.
[6] J. Cui, J. Tang, G. Shi, Z. Zhang, A fault feature extraction method of aerospace generator rotating rectifier based on improved stacked auto-encoder, Proc. Chin. Soc. Electr. Eng. 37 (19) (2017) 5696–5706.
[7] Z. Gao, C. Cecati, S.X. Ding, A survey of fault diagnosis and fault-tolerant techniques–part I: fault diagnosis with model-based and signal-based approaches, IEEE Trans. Ind. Electron. 62 (6) (2015) 3757–3767.
[8] Z. Gao, C. Cecati, S.X. Ding, A survey of fault diagnosis and fault-tolerant techniques–part II: fault diagnosis with knowledge-based and hybrid/active approaches, IEEE Trans. Ind. Electron. 62 (6) (2015) 3768–3774.
[9] V. Gomaty, S. Selvaperumal, Fault detection and classification with optimization techniques for a three-phase single-inverter circuit, J. Power Electron. 16 (3) (2016) 1097–1109.
[10] R. Guo, Z. Zhang, X. Liu, Exponential input-to-state stability for complex-valued memristor-based BAM neural networks with multiple time-varying delays, Neurocomputing 275 (2018) 2041–2054.
[11] H. Han, W. Lu, Y. Hou, J. Qiao, An adaptive-PSO-based self-organizing RBF neural network, IEEE Trans. Neural Netw. Learn. Syst. (2016), doi:10.1109/TNNLS.2016.2616413.
[12] G. Hinton, R. Salakhutdinov, Reducing the dimensionality of data with neural networks, Science 313 (5786) (2006) 504–507.
[13] G. Hinton, Where do features come from? Cognit. Sci. 38 (6) (2014) 1078–1101.
[14] F. Jia, Y. Lei, J. Lin, X. Zhou, N. Lu, Deep neural networks: a promising tool for fault characteristic mining and intelligent diagnosis of rotating machinery with massive data, Mech. Syst. Signal Process. 72–73 (2016) 303–315.
[15] Y. LeCun, Y. Bengio, G. Hinton, Review: deep learning, Nature 521 (2015) 436–444.
[16] B. Li, S. Shi, B. Wang, G. Wang, W. Wang, D. Xu, Fault diagnosis and tolerant control of single IGBT open-circuit failure in modular multilevel converters, IEEE Trans. Power Electron. 31 (4) (2016) 3165–3176.
[17] C. Li, R. Sanchez, G. Zurita, M. Cerrada, D. Cabrera, R.E. Vasquez, Multimodal deep support vector classification with homologous features and its application to gearbox fault diagnosis, Neurocomputing 163 (2015) 119–127.
[18] H. Liu, Z. Wang, B. Shen, X. Liu, Event-triggered H_∞ state estimation for delayed stochastic memristive neural networks with missing measurements: the discrete timecase, IEEE Trans. Neural Netw. Learn. Syst., doi:10.1109/TNNLS.2017.2728639. In press.
[19] R. Liu, Y. Li, X. Liu, Linear-quadratic optimal control for unknown mean-field stochastic discrete-time system via adaptive dynamic programming approach, Neurocomputing 282 (2018) 16–24.
[20] W. Liu, Z. Wang, X. Liu, N. Zeng, Y. Liu, F.E. Alsaadi, A survey of deep neural network architectures and their applications, Neurocomputing 234 (2016) 11–26.
[21] Y. Liu, Z. Wang, Y. Yuan, F.E. Alsaadi, Partial-nodes-based state estimation for complex networks with unbounded distributed delays, IEEE Trans. Neural Netw. Learn. Syst., doi:10.1109/TNNLS.2017.2740400. In press.
[22] C. Ma, X. Gu, Y. Wang, Fault diagnosis of power electronic system based on fault gradation and neural network group, Neurocomputing 72 (2009) 2909–2914.
[23] L. Ren, W. Wei, C. Gong, Q. Shen, Fault feature extraction technology for power devices in power electronic converters: a review, Proc. Chin. Soc. Electr. Eng. 35 (12) (2015) 3089–3101.
[24] H. Renaudineau, J.P. Martin, B. Nahid-Mobarakeh, S. Pierfederici, DC-DC converters dynamic modeling with state observer-based parameter estimation, IEEE Trans. Power Electron. 30 (6) (2015) 3356–3363.
[25] D.E. Rumelhart, G.E. Hinton, R.J. Williams, Learning representations by back--propagating errors, Nature 323 (1986) 533–536.
[26] M. Salah, K. Bacha, A. Chaari, H.B.M. El, Brushless three-phase synchronous generator under rotating diode failure conditions, IEEE Trans. Energy Convers. 29 (3) (2014) 594–601.
[27] H. Shao, H. Jiang, F. Wang, H. Zhao, An enhancement deep feature fusion method for rotating machinery fault diagnosis, Knowl. Based Syst. 119 (2017) 200–220.
[28] B. Shen, Z. Wang, H. Qiao, Event-triggered state estimation for discrete-time multi-delayed neural networks with stochastic parameters and incomplete measurements, IEEE Trans. Neural Netw. Learn. Syst. 28 (5) (2017) 1152–1163.
[29] B. Song, Z. Wang, L. Sheng, A new genetic algorithm approach to smooth path planning for mobile robots, Assem. Autom. 36 (2) (2016) 138–145.
[30] B. Song, Z. Wang, L. Zou, On global smooth path planning for mobile robots using a novel multimodal delayed PSO algorithm, Cognit. Comput. 9 (1) (2017a) 5–17.
[31] B. Song, Z. Wang, L. Zou, L. Xu, F.E. Alsaadi, A new approach to smooth global path planning of mobile robots with kinematic constraints, in: Proceedings of the International Journal of Machine Learning and Cybernetics, 2017, doi:10.1007/s13042-017-0703-7.
[32] W. Sun, S. Shao, R. Zhao, R. Yan, X. Zhang, X. Chen, A sparse auto-encoder-based deep neural network approach for induction motor faults classification, Measurement 89 (2016) 171–178.
[33] Z. Tian, X. Ge, An on-line fault diagnostic method based on frequency-domain analysis for IGBTs in traction PWM rectifiers, in: Proceedings of IEEE Eighth International Power Electronics and Motion Control Conference, 2016, pp. 3403–3407.
[34] P. Vincent, H. Larochelle, I. Lajoie, Y. Bengio, P. Manzagol, Stacked denoising autoencoders: learning useful representations in a deep network with a local denoising criterion, J. Mach. Learn. Res. 11 (12) (2010) 3371–3408.
[35] L. Wang, Z. Wang, G. Wei, F.E. Alsaadi, Finite-time state estimation for recurrent delayed neural networks with component-based event-triggering protocol, IEEE Trans. Neural Netw. Learn. Syst., doi:10.1109/TNNLS.2016.2635080. In press.
[36] R. Wang, Y. Zhan, H. Zhou, B. Cui, A fault diagnosis method for three-phase rectifiers, Int. J. Electr. Power Energy Syst. 52 (1) (2013) 266–269.
[37] R. Wang, Y. Zhan, H. Zhou, Application of s transform in fault diagnosis of power electronics circuits, Sci. Iran. D 19 (3) (2012) 721–726.
[38] Y. Wang, M. Liu, Z. Bao, Deep learning neural network for power system fault diagnosis, in: Proceedings of the Thirty Fifth Chinese Control Conference, 2016, pp. 6678–6683.
[39] F. Wu, J. Zhao, Current similarity analysis-based open-circuit fault diagnosis for two-level three-phase PWM rectifier, IEEE Trans. Power Electron. 32 (5) (2017) 3935–3944.
[40] F. Wu, J. Zhao, Y. Liu, D. Zhou, H. Luo, Primary source inductive energy analysis based real-time multiple open-circuit fault diagnosis in two-level three-phase PWM boost rectifier, IEEE Trans. Power Electron., doi:10.1109/TPEL.2017.2704589. In press.
[41] S. Yang, D. Xiang, A. Bryant, P. Mawby, L. Ran, P. Tavner, Condition monitoring for device reliability in power electronic converters: a review, IEEE Trans. Power Electron. 25 (11) (2010) 2734–2752.
[42] N. Zeng, H. Zhang, B. Song, W. Liu, Y. Li, A.M. Dobaie, Facial expression recognition via learning deep sparse autoencoders, Neurocomputing 273 (2018) 643–649.
[43] N. Zeng, Z. Wang, H. Zhang, F.E. Alsaadi, A novel switching delayed PSO algorithm for estimating unknown parameters of lateral flow immunoassay, Cognit. Comput. 8 (2) (2016) 143–152.
[44] N. Zeng, H. Zhang, Y. Li, J. Liang, A.M. Dobaie, Denoising and deblurring gold immunochromatographic strip images via gradient projection algorithms, Neurocomputing 247 (2017) 165–172.
[45] N. Zeng, Z. Wang, H. Zhang, W. Liu, F.E. Alsaadi, Deep belief networks for quantitative analysis of a gold immunochromatographic strip, Cognit. Comput. 8 (4) (2016) 684–692.
[46] L. Zou, Z. Wang, H. Gao, X. Liu, State estimation for discrete-time dynamical networks with time-varying delays and stochastic disturbances under the round-robin protocol, IEEE Trans. Neural Netw. Learn. Syst. 28 (5) (2017) 1139–1151.

Lin Xu received her B.S. degree in electrical information engineering in 2005, the M.S. degree in pattern recognition and intelligent system in 2008 both from Shandong University of Science and Technology, Qingdao, China. Now, she is pursuing her Ph.D. degree in pattern recognition and intelligent system at Shandong University of Science and Technology, Qingdao, China. She has been with Shandong University of Science and Technology as a lecturer since 2011. Her research interests include fractional order control, power electronics, robotics and deep neural network.

Maoyong Cao received the B.S. degree in physics from Nankai University, China, in 1986, the M.S. degree in control theory and control engineering from the Shandong University of Science and Technology (SDUST), China, in 1993, and the Ph.D. degree in optical engineering from Tianjin University, China, in 2002. He was a Visiting Scholar in Germany for several months. He is currently the Leader of the Institute of Image Processing and Pattern Recognition at SDUST. He has led more than ten projects, including the National Natural Science Foundation of China and the Natural Science Foundation of Shandong Province. He has published more than 60 papers and several monographs. His research interests mainly focus on image processing, machine vision, detection, monitoring, and automation.

Baoye Song received the B.S. degree in automation in 2005, the M.S. degree in control theory and control engineering in 2008 both from Qingdao University of Science and Technology, Qingdao, China, and the Ph.D. degree in control theory and control engineering in 2011 from Shandong University, Jinan, China. He has been with Shandong University of Science and Technology as a lecturer since 2011. His research interests include nonlinear filtering, intelligent optimization algorithm, robotics and fault diagnosis.

Jiansheng Zhang received his B. S. degree in electrical information engineering from Qingdao University, Qingdao, China, in 2011. He is currently pursuing his M.S. degree in electrical engineering and automation at Shandong University of Science and Technology, Qingdao, China. His research interests include big data analysis and deep learning techniques.

Yurong Liu was born in China in 1964. He received his B.Sc. degree in Mathematics from Suzhou University, Suzhou, China, in 1986, the M.Sc. degree in Applied Mathematics from Nanjing University of Science and Technology, Nanjing, China, in 1989, and the Ph.D. degree in Applied Mathematics from Suzhou University, Suzhou, China, in 2001. He is currently a professor with the Department of Mathematics at Yangzhou University, China. He also serves as an Associate Editor of Neurocomputing. So far, he has published more than 50 papers in refereed international journals. His current interests include stochastic control, neural networks, complex networks, nonlinear dynamics, time-delay systems, multi-agent systems, and chaotic dynamics.

Fuad E. Alsaadi received the B.S. and M.Sc. degrees in electronic and communication from King Abdulaziz University, Jeddah, Saudi Arabia, in 1996 and 2002, respectively. He received the Ph.D. degree in optical wireless communication systems from the University of Leeds, Leeds, U.K., in 2011. Between 1996 and 2005, he worked in Jeddah as a Communication Instructor at the College of Electronics and Communication. He is currently an Assistant Professor in the Department of Electrical and Computer Engineering within the Faculty of Engineering, King Abdulaziz University, Jeddah, Saudi Arabia. He published widely in the top IEEE communications conferences and journals. His research interests include optical systems and networks, signal processing, synchronization, and systems design. He received the Carter award, University of Leeds for the best Ph.D.